Effect of active phenolic acids on properties of PLA-PHBV blend films

Eva Hernández-García , María Vargas [*] , Amparo Chiralt

Departamento de Tecnología de Alimentos, Instituto Universitario de Ingeniería de Alimentos para el Desarrollo, Universitat Politècnica de València, Spain

ABSTRACT

Phenolic acids (ferulic, *p*-coumaric, and protocatechuic) have been incorporated into polylactic (PLA): Poly(3-hydroxybutyrate-co-3-hydroxyvalerate) (PHBV) (75:25) blend films that were obtained by melt-blending and compression moulding, using PEG1000 as a plasticizer. Film microstructure, thermal behavior, functional properties, and release kinetics of phenolic acids in different food simulants were analyzed, and the film anti-microbial activity against *Listeria innocua*. Phenolic acids led to an increase in the glass transition temperature of PLA while PHBV supercooling occurred in the films containing protocatechuic acid, which affected their thermal degradation behavior. Polymer matrices with phenolic acids were stiffer and more resistant to break than the polyester blend, but with similar extensibility, while oxygen and water vapor barrier capacity were also improved, especially in films containing protocatechuic acid. The release rate and ratio of phenolic acids increased when the polarity of the food simulant decreased, although very slow delivery was observed in all cases. The limited release of active compounds in aqueous media provoked that films did not significantly inhibit the growth of *Listeria innocua* in inoculated culture medium.

1. Introduction

In the last few years, there has been a trend to reduce as much as possible the addition of synthetic preservatives in food products while consumers demand healthy and easy-to-prepare foods with high nutritional value (Dıblan & Kaya, 2018). In order to face this challenge and avoid deteriorating processes in food, active packaging materials are being developed. These materials can incorporate compounds that absorb or release substances from or on the packaged foods or in the head-space of the container (Malhotra et al., 2015). In this sense, the use of active packaging films has been proved to be an alternative to maintain food quality and extend its shelf-life (Esmaeili et al., 2020; Moreno et al., 2018; Ngo et al., 2020; Szabo et al., 2020) at the same time that the drawbacks associated with the direct application of active compounds in the food product surface are reduced (Castillo et al., 2017). To increase the shelf-life and maintain the storage-keeping quality of the packaged foods, active compounds such as essential oils (Esmaeili et al., 2020; Jiang et al., 2020; Krepker et al., 2017; Zhang et al., 2020; Figueroa-Lopez et al., 2020), organic acids (Narasagoudr et al., 2020; Sharma et al., 2020; Wang et al., 2020), and plant extracts (Choulitoudi et al., 2020; Szabo et al., 2020), among others, have been incorporated into active films. Within organic acids, phenolic acids have been shown to have significant antimicrobial and antioxidant properties (Moreno et al., 2006; Porras-Loaiza & López-Malo, 2009).

Phenolic acids consist of an aromatic ring and at least one hydroxyl substituent. They are found in plant tissues, foods, and metabolites (Badui Dergal, 2006). Phenolic acids, such as ferulic acid, *p*-coumaric acid, and protocatechuic acid, have noticeable antimicrobial and antioxidant activity. These phenolic acids are the main compounds of aqueous extracts from lignocellulosic residues, such as those obtained from some agri-food industries, which can be used as a source of active components for their use in active packaging materials, following the principles of the circular economy. Ferulic acid showed an inhibitory effect against *Listeria monocytogenes* (Takahashi et al., 2013, 2015), and its incorporation by solvent casting methods into blend poly (lactide)-poly(butylene adipate-co-terephthalate) (PLA-PBAT) was effective against *Listeria monocytogenes* and *Escherichia coli* (Sharma et al., 2020). *P*-coumaric acid is effective against different bacteria (Lou et al., 2012), such as *Enterobacteriaceae* (Mitani et al., 2018) and *E. coli* and *Staphylococcus aureus* (Contardi et al., 2019). Protocatechuic acid inhibited the growth of *Listeria monocytogenes* in cream cheese (Stojković et al., 2013) and of *E. coli, S.* Typhimurium*, L. monocytogenes, S. aureus,* and *B. cereus* in ground beef and apple juice (Chao & Yin, 2009).

As concerns the development of new food packaging materials, one of the techniques recently used to improve their functional properties is the combination of two or more polyesters in the production phase

(Kanda et al., 2018). This strategy, which is cheaper and more rapid than the use of new monomers and new polymerization routes, allows for obtaining films with improved properties as compared to pure polymer films. However, the improvement of one property can weaken another (Zhang et al., 2012). For example, PLA-based films show low ductility and high permeability to water vapor and O_2 (Auras et al., 2004), and to overcome these drawbacks, PLA has been blended with a highly crystalline biopolymer with a high melting point such as PHB (Noda et al., 2004). Previous studies have reported an improvement in the crystallization of PLA due to the positive effect of PHB/PHBV crystals (Arrieta et al., 2019; Liu et al., 2015; Zembouai et al., 2013), thus improving the water vapor and oxygen barrier properties (Zembouai et al., 2013), the thermal stability and mechanical resistance (Liu et al., 2015) as compared to pure PLA films. In the same sense, Requena et al. (2018) obtained compression-molded PLA:PHBV (75:25) blend films, with 15% PEG1000, with improved extensibility and water barrier capacity. However, to the best of our knowledge, phenolic acids have not been incorporated into thermoplastic PLA-PHBV blend films to develop active packaging materials.

This study aimed to analyze the functional properties of PLA-PHBV blend films obtained by melt-blending and compression molding incorporating phenolic acids (ferulic, *p*-coumaric, and protocatechuic) as antibacterial compounds. The antibacterial effectiveness of the films against *L. innocua* and the release kinetics of the phenolic acids in different food simulants have also been analyzed.

2. Materials and methods

2.1. Materials

Poly(3-hydroxybutyrate-co-3-hydroxyvalerate) (PHBV) ENMAT Y1000P with 3% hydroxyvalerate was supplied by Helian Polymers B.V. (Belfeld, Holland). Amorphous PLA 4060D, density of 1.24 g/cm^3 and average molecular weight of 106,226 D with 40% of low molecular weight fraction (275 D) as reported by Muller, González-Martínez, and Chiralt (Muller et al., 2017) was purchased from Natureworks (U.S.A). The plasticizer poly(ethylene glycol) with a molecular weight of 1000 Da (PEG1000), with a solubility in water of was purchased from Sigma-Aldrich (Steinheim, Germany). Ferulic, *p*-coumaric, and protocatechuic acids were purchased from Sigma-Aldrich (Madrid, Spain). UV methanol, UV ethanol, phosphorus pentoxide (P_2O_5), and magnesium nitrate-6-hydrate ($Mg(NO_3)_2$) were supplied by Panreac Química, S.A. (Castellar del Vallès, Barcelona, Spain).

2.2. Preparation of blend films

PLA-PHBV blend films were obtained by melt blending and compression moulding in a polymer ratio of 75:25, using PEG1000 (15 g/100 g polymer) as a plasticizer, and without or with a constant amount of antibacterial compound (ferulic, *p*-coumaric, and protocatechuic acids) of 2% (w/w) with respect to the polymer matrix (polymer plus plasticizer). The ratio of polymers and PEG1000, as the plasticizer, were selected on the basis of previous studies (Requena et al., 2016; Requena et a., 2018). This concentration in the films was selected on the basis of the minimal inhibitory concentration (MIC) of the compounds against several bacteria (in the range of 1 g/L) in order to exceed the MIC values in the test medium if a complete release occurs from the film. The melt blending process was carried out in an internal mixer (HAAKE™ PolyLab™ QC, Thermo Fisher Scientific, Germany) at 170 °C and 50 rpm for 12 min. The obtained pellets were conditioned at 25 ºC and 53% RH. Four grams of the conditioned pellets were put onto Teflon sheets and preheated at 200 ºC for 5 min in a hot-plate press (Model LP20, Labtech Engineering, Thailand). Films were obtained by compressing at 200 °C for 4 min at 100 bars and a final cooling cycle for 3 min until the temperature reached about 70 ºC (Requena et al., 2018). The obtained films were conditioned at 25 ºC and 53% RH.

The thickness of the films was measured in triplicate in six random points of each sample by a hand-held digital micrometer (Electronic Digital Micrometer, Comecta S.A., Barcelona, Spain).

2.3. Microstructural and thermal analyses

The microstructure of films was observed by Field Emission Scanning Electron Microscope (FESEM Ultra 55, Zeiss, Oxford Instruments, UK). The samples were maintained with P_2O_5 for two weeks to ensure the total dehydration of the films. Film samples were cryofractured with liquid nitrogen to obtain cross-sections, which were mounted on support stubs and coated with platinum prior performing the microstructural observations at 2 kV.

Differential scanning calorimetry analyses were carried out using a Differential Scanning Calorimeter (DSC823^e Star^e Mettler-Toledo Inc., Switzerland). Films samples (10 mg) were placed into aluminum pans and tightly sealed. Samples were heated from room temperature to 180 ºC at 10 ºC/min. Then, samples were cooled until − 30 ºC at 50 ºC/min and heated again to 180 ºC at 10 ºC/min, as reported by Requena et al. (2018). As a reference, an empty aluminum pan was used. Each sample was analyzed in duplicate.

The thermal stability was analyzed using a thermogravimetric analyzer (TGA 1 Star^e System analyzer, Mettler-Toledo, Switzerland) by sample heating from 25 to 600 ºC at 10 ºC/min under nitrogen flow (10 mL/min). Samples (3 mg maximum) were conditioned in desiccators with P_2O_5, using at least two replicates per formulation. In each test, the corresponding mass curve was obtained as a function of temperature. From these curves, the derived curves (DTG) were obtained as a function of temperature, and the corresponding values of T_{onset} (initial degradation temperature) and T_{max} (temperature of maximum degradation rate) using the STAR^e Evaluation Software (Mettler-Toledo, Switzerland).

2.4. Tensile properties and thickness

Mechanical properties (elastic modulus (EM), tensile strength (TS), and elongation at break (E) were determined using a Universal Testing Machine (Stable Micro System TA. XT plus, Haslemere, England), according to ASTM standard method D882 (ASTM, 2001). EM, TS, and E were determined from the stress strain curves, estimated from force-distance data obtained for eleven pre-conditioned (53% RH and 25 ºC) film samples of each formulation (2.5 cm wide and 10 cm long), which were mounted in the extension grip of the equipment and stretched at 50 mm·min^{-1} until breaking.

2.5. Barrier properties

The oxygen permeability (OP) was determined using OX-TRAN equipment (Model 1/50, Mocon, Minneapolis, USA). Two film samples per formulation were previously conditioned at 53% RH and 25 ºC (ASTM, 2002). The tests were performed at 53% RH, and the film exposure area was 50 cm^2. OP was calculated by dividing the oxygen transmission rate by the difference in the oxygen partial pressure between the two sides of the film and multiplying by the film thickness.

The water vapor permeability (WVP) of films was measured according to a modification of the ASTM E96–95 (ASTM, 1995) gravimetric method, at 25 ºC and a RH gradient of 53%− 100% using Payne permeability cups (Elcometer SPRL, Hermelle/s Argenteau, Belgium) of 3.5 cm in diameter. This gradient was generated by using an oversaturated $Mg(NO_3)_2$ solution and pure water, respectively. Three circular samples of each formulation were prepared, and the thickness of each sample was measured in six random points with an electronic digital micrometer (Comecta S.A., Barcelona, Spain). To determine WVP, the cups were weighed periodically using an analytical balance (ME36S, Sartorius, Germany; ±0.00001 g) at intervals of 1.5 h for 24 h after the steady-state had been reached. The slope of the weight loss

versus time was plotted, and the water vapor transmission rate (WVTR) and water vapor permeability were calculated according to Vargas et al. (2009).

2.6. Optical properties

The optical properties (transparency and CIE-L*a*b* color coordinates) were determined in triplicate by measuring the reflection spectrum of the samples using a Konica Minolta spectrocolorimeter, model CM-5 (Minolta CO., Tokyo, Japan). The transparency of the films was determined using the internal transmittance (T_i), applying the Kubelka-Munk theory (Hutchings, 1999) for multiple scattering to the reflection spectra (400–700 nm), given the reflection spectra of both black and white backgrounds. The CIE-L*a*b* color coordinates were obtained from the reflectance of an infinitely thick material layer by considering illuminant D65 and observer 10°. Psychometric coordinates Chroma (C_{ab}*) and hue (h_{ab}*) were also determined using Eqs. (1) and (2) (Hutchings, 1999).

$$h_{ab}* = \arctan(b^*/a^*) \qquad \text{Eq. (1)}$$

$$cab* = \sqrt{(a^*)^2 + (b^*)^2} \qquad \text{Eq. (2)}$$

Moreover, to evaluate the color differences between ferulic, *p*-coumaric, and protocatechuic films and the control film, the following equation was used Eq. (3):

$$\Delta E = \sqrt{(\Delta L^*)^2 + (\Delta a^*)^2 + (\Delta b^*)^2} \qquad \text{Eq. (3)}$$

The film gloss was determined at an incidence angle of 60°, according to the ASTM standard method D523 (ASTM, 1999), using a flat surface gloss meter (Multi Gloss 268, Minolta, Germany). Measurements of each sample were taken in triplicate, and three films of each formulation were considered. All results are expressed as gloss units (GU), relative to a highly polished surface of black glass standard with a value near 100 GU.

2.7. Retention of active compounds and release kinetics in different food simulants

The final phenolic acids content in the films was determined by methanol extraction, followed by spectrophotometric quantification using a UV–visible spectrophotometer (Thermo Scientific Evolution 201, EEUU). Standard calibration curves for ferulic, *p*-coumaric, and protocatechuic acids were obtained to determine their concentration from the absorbance values using an initial solution with 500 µg·mL^{-1} and subsequent dilutions. Ferulic, *p*-coumaric, and protocatechuic acids were quantified through absorbance measurements at 320, 309, and 208 nm, respectively, using the methanol extract of active-free PLA-PHBV films as a blank solution. Films samples of 100 mg were cut in strips and placed in flasks with 10 mL of UV methanol, under stirring for 48 h at 20 °C. After that, samples were filtered and appropriately diluted to obtain absorbance values between 0.2 and 0.8. All analyses were carried out in samples from four different positions of four different films to analyze the degree of homogeneity of the active distribution throughout the film.

In the release studies two different food simulants were used: 10% (v/v) (simulant A) and 50% (v/v) (simulant D1) ethanol-water solutions (Commission regulation (EU) 10/2011). 500 mg of each sample was placed into a flask containing 100 mL of each simulant. Thereby, each film formulation-food simulant system was kept under stirring at 25°C throughout the assay time, using a spectrophotometric method. For simulant A, absorbance was measured at 311, 287, and 291 nm, where the ferulic, *p*-coumaric, and protocatechuic acid absorbance is maximum, respectively. For simulant D1, measurements were performed at 313, 290, and 293 nm, where the ferulic acid, *p*-coumaric, and protocatechuic acid absorbance is maximum, respectively. Phenolic acid

quantification in the liquid phase was established using each simulant's previously obtained calibration curves. The assay was performed in triplicate.

Two empirical models were considered to describe the behavior of the active compounds in the food simulants. To predict the release kinetics, the Peleg model was applied (Eq.4) (Peleg, 1988).

$$\frac{t}{Mt} = k_1 + k_2 t \qquad \text{Eq. (4)}$$

where: M_t is the total active compound released into the simulants after contact time t; k_1 and k_2 are the model constants, where $1/k_1$ is the release rate at the beginning of the process, and $1/k_2$ is the mass of active compound released at equilibrium (M_∞). In addition, the experimental results were fitted to the Korsmeyer-Peppas model (Eq. 5) (Siepmann & Peppas, 2011) to investigate the possible coupling of the relaxation of the polymer in contact with the solvent with de diffusion of the active compound through the polymer matrix.

$$\frac{Mt}{M\infty} = kt^n \qquad \text{Eq.(5)}$$

where: M_t/M_∞ is the fraction of active compound at time t (h); k is the rate constant of the film (h^{-n}); n is the diffusional exponent that provides information about the mechanisms involved in the release process, which takes values in the 0–1 interval (dimensionless). Thus, a 0.5 value for the diffusional exponent means that the release occurs through Fickian diffusion, whereas if the n value is higher than 0.5 (anomalous transport), the diffusion and the polymer relaxation rates are coupled. If the n value is lower than 0.5, a quasi-Fickian diffusion for the active release can be considered (Siepmann & Peppas, 2012).

2.8. Antibacterial activity

The minimum inhibitory concentration of ferulic, *p*-coumaric, and protocatechuic acids was determined as described by Requena et al. (2019). *Listeria innocua* (CECT 910, Spanish Type Culture Collection, Burjassot, València) and *E. coli* (CECT 101, Spanish Type Culture Collection Burjassot, València) stored at − 25 °C with 30% glycerol, have been used. *Listeria innocua* strains have been previously used to model the food-borne pathogen *L. monocytogenes* in inactivation experiments (Mohan et al., 2019).

Bacterial cultures in the exponential growth phase were prepared by inoculating the microbial stock suspensions into TSB, followed by incubation at 37 °C for 24 h. The inocula were diluted in TSB tubes to get a target inoculum of 10^5 colony-forming units mL^{-1}. Aliquots of 100 µl were taken from this bacterial suspension and deposited in each of the wells of the 96-well-plate. In parallel, stock solutions of the different active compounds were prepared in DMSO with a 3 mg active/ mL concentration. Thus, 100 µl of each of the solutions with the active ingredients were transferred to different positions of the previously identified multiwell plate and incubated for 24 h at 37 °C. Certain positions of the plate were used to control the test. After 24 h of incubation, a solution of the MTT reagent was prepared in PBS (5 mg/ mL), and 10 µl was added to each well of the plate. The plate was incubated again for 4 h at 37 °C, and after this time, the results were visually read. The MIC of each active compound was the lowest concentration at which no color change (microbial growth) occurred.

The antibacterial effect of PLA-PHBV blend films containing the polyphenol acids was evaluated in vitro (liquid medium test) according to the methodology described Valencia-Sullca et al. (2016), with some modifications. *Listeria innocua* (CECT 910, Spanish Type Culture Collection, Burjassot, València) stored at − 25 °C with 30% glycerol has been used. Bacterial cultures of *Listeria innocua* in the exponential growth phase were prepared as described below. The inoculum were diluted in TSB tubes to get a target inoculum of 10^4 colony-forming units mL^{-1}. Film samples of 5.86 × 9 cm (ferulic and protocatechuic acid)

and 7.54 × 9 cm (*p*-coumaric acid) obtained from the different types of film formulation were placed in TSB tubes. Inoculated tubes without film were used as control samples. Immediately after the inoculation and after 6 days at 10 ºC, the microbial counts on plates were determined. Serial dilutions were made and poured onto Base Palcam agar medium dishes (which contained the selective supplement for *Listeria*), incubated for 48 h at 37 ºC. All tests were run in triplicate.

2.9. Statistical analysis

Statgraphics Centurion XVII-64 software (Manugistics Corp., Rockville, Md.) was used to conduct statistical analyses through a variance analysis (ANOVA). Homogeneous sample groups were obtained by using the LSD test (95% significance level).

3. Results and discussion

3.1. Microstructure and thermal behavior

Microstructural images show the degree of homogeneity in the distribution of film matrix components, a factor related to the material's functional properties. The cross-section morphologies of PLA-PHBV blend films and PLA-PHBV blend films containing ferulic acid, *p*-coumaric acid, and protocatechuic acid are shown in Fig. 1.

In the cross-section of PLA-PHBV films (P), a lack of miscibility between the polyesters and the plasticizer can be observed, with different domains of PLA and PHBV, as previously reported (Hernández-García et al., 2021; Requena et al., 2018). This polymer phase separation was not predicted by the Hildebrand solubility parameters (δ: 20.8 MPa$^{1/2}$, 20.2 MPa$^{1/2}$ and 19.2 MPa$^{1/2}$, respectively for PEG, PLA and PHBV), which suggested good miscibility between components ($\Delta\delta <$ 2 MPa$^{1/2}$), as reported by other authors (Quiles-Carrillo et al., 2018; Snowdon et al., 2017). This could be attributed to the great tendency of PHBV to crystalize.

The incorporation of phenolic acids led to a more heterogeneous cross-section, where a more brittle fracture was observed in different domains, in contrast with that observed by Mathew and Abraham

(2008) for starch-chitosan blend films containing ferulic acid. In all cases, small particles dispersed in the polymer matrix were observed, attributed to dispersed aggregates of phenolic acids, thus evidencing the lack of complete miscibility of these compounds with the polymers. The latter was particularly evident in films containing protocatechuic acid that showed aggregates of larger size.

Table 1 shows the results obtained from DSC analysis: glass

Table 1
Thermal properties of PLA-PHBV blend films (P) and PLA-PHBV blend films containing ferulic acid (P-F), *p*-coumaric acid (P-C), and protocatechuic acid (P-P) from the first and the second heating scan: Glass transition (T_g), melting temperature (T_m) and melting enthalpy (ΔH_m) of the polymers in the blend. Mean values ± standard deviation.

First Heating Scan			
Formulation	$T_{g\ PLA}$ (ºC)	$T_{m\ 1}$ (ºC)	$T_{m\ 2}$ (ºC)	ΔH_m (J/g polymer)
P	36.1 ± 1.3[d]	162.0 ± 3.0[a]	169.1 ± 1.7[a]	20 ± 4[ab]
P-F	39.4 ± 0.3b[c]	154.2 ± 0.6[b]	163.5 ± 0.4[b]	18.9 ± 1.0[b]
P-C	46 ± 0.0[a]	158.8 ± 1.4[a]	167.4 ± 1.7[a]	20.3 ± 1.6[b]
P-P	41 ± 0.3[b]	–	163.8 ± 0.3[b]	24 ± 2[a]

Second Heating Scan			
	$T_{g\ PLA}$ (ºC)	$T_{m\ 1}$ (ºC)	$T_{m\ 2}$ (ºC)	ΔH_m (J/g polymer)
P	29.1 ± 0.1[d]	163.0 ± 2.0[a]	170.0 ± 2.0[a]	18.6 ± 3.0[ab]
P-F	33.9 ± 0.7[c]	154.0 ± 0.3[c]	162.0 ± 0.1[c]	19.4 ± 0.7[b]
P-C	37 ± 0.0[a]	159.3 ± 1.9[b]	165 ± 2[b]	21.4 ± 1.0[a]
P-P	36.4 ± 0.2[b]	–	162.9 ± 0.3[b]	22.4 ± 1.6[a]

T_m ferulic (ºC): 172.54; T_m *p*-coumaric (ºC): 214.9; T_m protocatechuic (ºC): 199.15
Different superscript letters (a-c) within the same column indicate significant differences among formulations (p < 0.05).
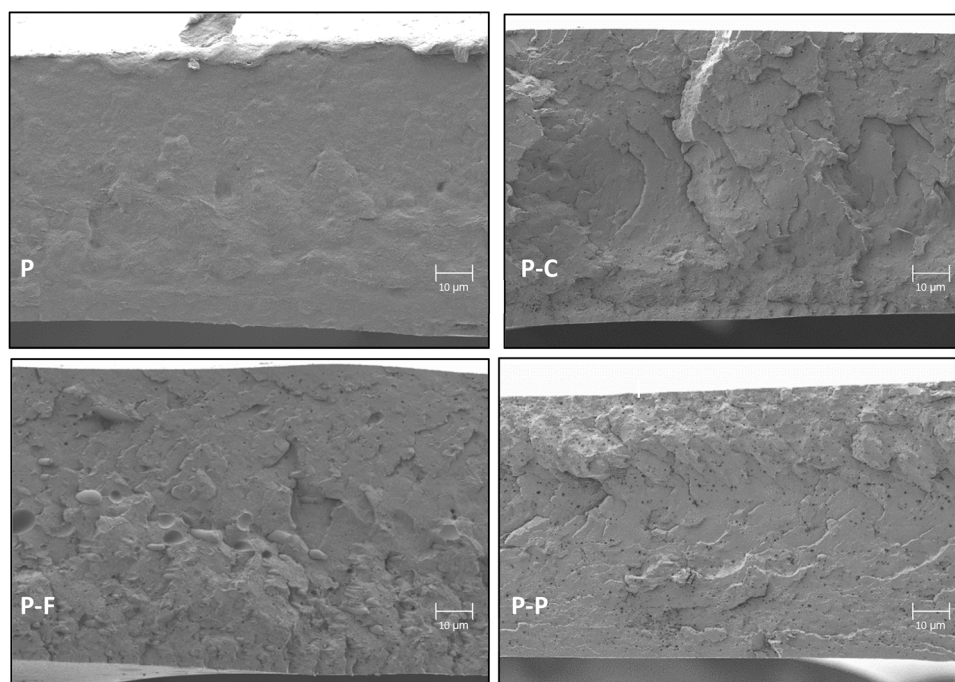

Fig. 1. Field Emission Scanning Microscope (FESEM) micrographs of the cross-section of PLA-PHBV blend films (P) and PLA-PHBV blend films containing ferulic acid (P-F), *p*-coumaric acid (P-C), and protocatechuic acid (P-P) (magnification: 650X; bar: 10 μm).

transition temperature (T_g), melting temperature (T_m), and melting enthalpy (ΔH_m) of PLA-PHBV active films as deduced from 1st heating scan and the second heating scan when the thermal history of the polymers was erased (Table 1). In Fig. 2, the DSC curves from the 1st and the 2nd heating scan are shown.

In both first and second heating scans, a two-peak endothermic event was observed for the polymers at about 160 and 170 °C, as observed by Requena et al. (2018) for similar blend films with PLA and PHBV. Only the films containing protocatechuic acid showed a single endothermic peak at 163 °C, also observed in some films with a similar PLA/PHBV ratio. Moreover, these films containing protocatechuic acid exhibited an exothermic peak around 75–80 °C during both scans, which suggests that supercooling of PHBV was promoted in the presence of proto-catechuic acid and, as a consequence, PHBV crystalized after glass transition in the PLA matrix. Considering the slower crystallization of PLA, mainly in the amorphous form used, there are two possibilities for the origin of the two melting peaks: the melting and subsequent crystallization of the PHBV or the formation of two types of lamellae structures in the crystals, as speculated by Furukawa et al. (2005) by analyzing the crystallization behavior of PHB in different blends with PLA. In fact, the total melting enthalpy values are very close in all film formulations (19–22 J/g), which considering the mass fraction of PHBV in the blend and the melting enthalpy of pure PHBV (146 J/g PHBV, (González-Ausejo et al., 2017) represent a crystallinity degree of PHVB of about 55%. However, in the films containing protocatechuic acid, this crystallinity was only reached after heating the films, and much fewer crystalline forms would be present in the supercooled obtained film. The incorporation of ferulic and *p*-coumaric acids slightly decreased the melting points of PHBV, with no significant changes in the total melting enthalpy, which showed values in the range reported by Requena et al. (2018) for similar polymer blends. This reduction reflects the specific interactions between phenolic acid and PHBV, such as hydrogen bonds between phenolic hydroxyls and polyester carbonyls, which slightly reduces the size of crystals and melting point. In the case of proto-catechuic acid, these interactions promoted the polymer supercooling without total crystallization in the film, but only when the temperature increased above the T_g of the PLA matrix. This behavior suggests that protocatechuic acid could establish stronger interactions with the polymers that affected the crystallization behavior in the matrix. The particular molecular structure of protocatechuic acid (Table 4) could be more able to promote interchain hydrogen bonds, enhancing the cross-linking effect, thus inhibiting crystallization because of the more limited molecular mobility. This inhibition was also reflected in the T_g values of PLA commented below. The reduction of melting points due to the addition of *p*-coumaric acid was also observed by Contardi et al. (2019) in polyvinylpyrrolidone films.

The glass transition of PHBV was not recorded in the DSC analyses due to the low expected value (−1 °C, Ferreira et al., 2002) that could not be evaluated with the used equipment. For the PLA phase, the T_g values were 36 °C for the first scan and 29 °C for the second scan, which agreed with those previously reported by Requena et al. (2018) for similar polymer blends. The relaxation enthalpy associated with the endothermic peak in the glass transition region was observed in the first heating scan for P-P and P-C films due to the aging effects. The incorporation of phenolic acids led to increased T_g values, especially for coumaric and protocatechuic acids, which exert an anti-plasticizing effect in the PLA:PHBV matrix. As previously pointed out, this could be due to the promotion of interchain interactions through hydrogen bonds between phenolic hydroxyls and carbonyl of polyesters, thus reducing the molecular mobility in the matrix and increasing the T_g. The ability of each acid to promote interchain associations will be affected by the molecular structure of phenolic acid (shown in Table 4). In contrast, Kasmi, Gallos, Beaugrand, Paës, and Allais (Kasmi et al., 2019) use synthesized ferulic acid derivatives (without hydroxyl groups) as plasticizers in PLA.

The effect of phenolic acids on the thermal degradation pattern of PLA: PHBV blends is shown in Fig. 3. All films exhibited two different degradation steps that can be attributed to the separated degradation of each polyester, PLA and PHBV, according to the lack of polymer miscibility previously reported (Armentano et al., 2015; Requena et al., 2018), being PLA more thermostable than PHBV as reported by Ferreira et al. (2002) and Zhao et al. (2013). The initial degradation temperatures (T_{onset}) and the temperature at the maximum degradation rate (T_{peak}) for the different degradation steps of the polyester blend films containing or not phenolic acids are shown in Fig. 3.

The peak temperatures are at around 267 °C and 321 °C and can be attributed to the PHBV and PLA maximum degradation rates, respectively. Incorporating phenolic acids into the polymeric matrix provoked different effects on thermal behavior. Ferulic and coumaric acids led to a significant increase ($p > 0.05$) in the initial degradation temperatures of the polymer blends. However, this effect was not observed with the addition of protocatechuic acid, which caused a decrease in the thermal stability of the blends, decreasing both the onset temperature and those of the maximum degradation rates of PHBV and PLA. These changes in thermal degradation behavior are coherent with the described patterns for glass transition and crystallization deduced from DSC analyses. Degradation temperature increases when the cohesive forces in the matrix arise, which are affected by the cross-linking and crystallization degree in the matrix. The described cross-linking effect promoted by phenolic acids could explain the slight delay in the onset of thermal degradation of polyesters when ferulic, and coumaric acid were added. In contrast, protocatechuic acid inhibited PHBV crystallization, and therefore thermo-degradation occurred at lower temperatures.

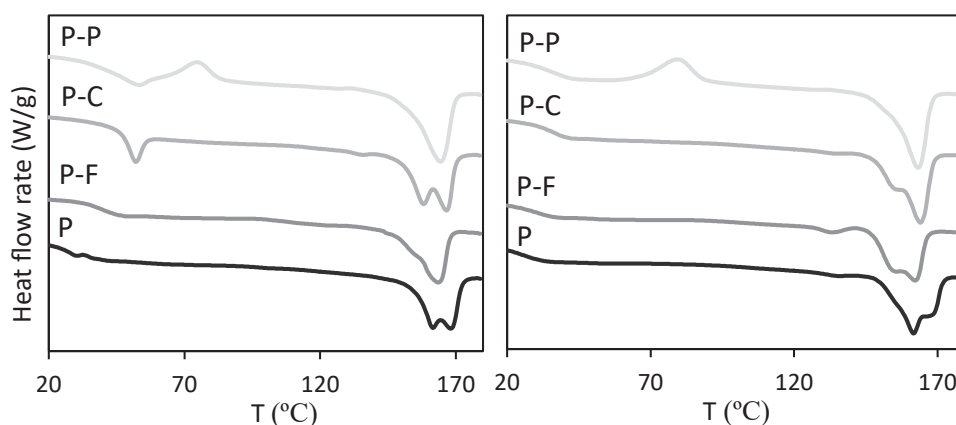Microstructural and thermal analyses revealed that PLA, PHBV, and

Fig. 2. DSC thermograms of PLA-PHBV blend films (P) and PLA-PHBV blend films containing ferulic acid (P-F), *p*-coumaric acid (P-C), and protocatechuic acid (P-P) obtained from the first heating scan (left) and the second heating scan (right).
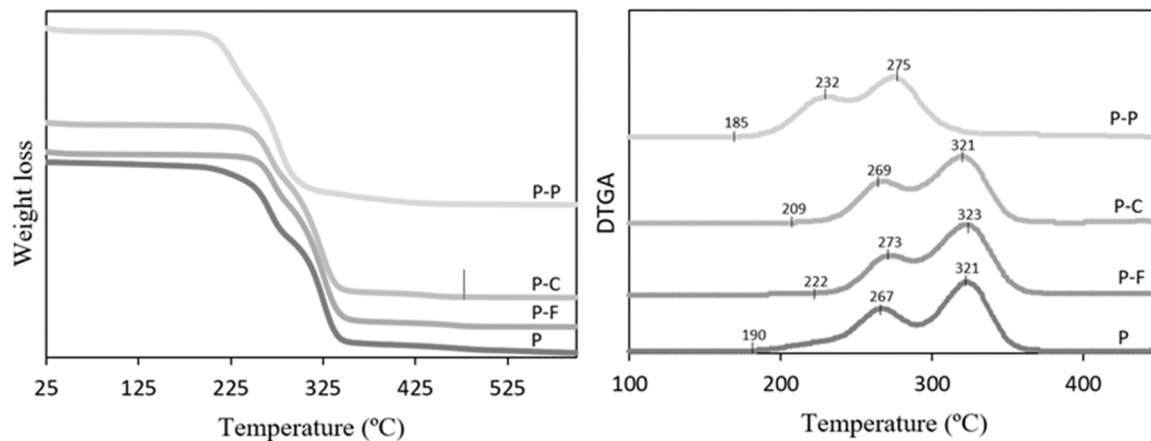
Fig. 3. Thermogravimetric analysis (TGA) and DGTA curves (initial degradation temperature (T_{onset}) and the temperature at the maximum degradation rate (T_{peak}) for the main steps of PLA-PHBV blend films (P) and PLA-PHBV blend films containing ferulic acid (P-F), *p*-coumaric acid (P-C), and protocatechuic acid (P-P)).

phenolic acids are not completely miscible, but interchain interactions occurred probably due to the interchain hydrogen bonds and phenolic molecules. The latter modifies the molecular mobility in the matrix, giving rise to an increase in the Tg and changes in the polymer crystallization pattern, affecting the polymers' thermal stability. Protocatechuic acid seems to promote the strongest interactions, enhancing the Tg value and limiting the crystallization of PHBV. In contrast, the lack of crystallization in protocatechuic acid-containing films makes the PHBV matrix less thermostable (Nuchanong et al., 2021).

3.2. Tensile properties and film thickness

The thickness values of the films are shown in Table 2. The incorporation of *p*-coumaric acid did not have a significant effect (p > 0.05) on film thickness, but ferulic acid led to an increase in film thickness,

Table 2
Tensile properties (Elastic modulus: EM, tensile strength: TS and deformation at break: %E), thickness, barrier properties (water vapor, WVP, and oxygen, OP, permeability), color parameters, total color difference as regards P film (ΔE), gloss and internal transmittance (T_i) at 550 nm of PLA-PHBV blend films (P) and PLA-PHBV blend films containing ferulic acid (P-F), *p*-coumaric acid (P-C) and protocatechuic acid (P-P). Mean values ± standard deviation.

	P	P-F	P-C	P-P
EM (MPa)	1050 ± 90[c]	1112 ± 100[bc]	1176 ± 50[ab]	1231 ± 90[a]
TS (MPa)	19.0 ± 1.5[b]	23.0 ± 1.9[a]	23.0 ± 2.3[a]	24.5 ± 3.6[a]
E (%)	2.3 ± 0.2[a]	2.4 ± 0.4[a]	2.2 ± 0.3[a]	2.3 ± 0.4[a]
Thickness (μm)	145 ± 0.015[b]	155 ± 0.018[a]	143 ± 0.016[b]	138 ± 0.018[c]
WVP (g.mm.kPa^{-1}.h^{-1}. m^{-2})	0.21 ± 0.05[a]	0.16 ± 0.01[ab]	0.18 ± 0.02[ab]	0.14 ± 0.01[b]
OPx10^{14} (cm^3·m^{-1}·s^{-1}·Pa^{-1})	168 ± 0.3[a]	149 ± 10[b]	122 ± 1.6[c]	110 ± 7.7[c]
L*	77.0 ± 0.9[b]	78.7 ± 0.7[a]	78.0 ± 0.5[a]	76.7 ± 0.5[b]
h_{ab}*	82.5 ± 0.8[b]	82.5 ± 0.6[b]	83.8 ± 0.5[a]	81.6 ± 0.4[c]
C_{ab}*	14.8 ± 0.5[a]	14.1 ± 0.6[b]	14.6 ± 0.3[ab]	13.5 ± 0.4[c]
ΔE	–	1.74 ± 0.1[a]	1.03 ± 0.1[b]	1.37 ± 0.3[ab]
Gloss 60º	12.4 ± 1.3[d]	18.9 ± 2.9[c]	23.6 ± 2.3[a]	21.6 ± 3.2[b]
T_i (λ = 550 nm)	80 ± 0.01[c]	82 ± 0.01[b]	83 ± 0.01[a]	83 ± 0.01[a]

Different superscript letters (a-d) within the same column indicate significant differences among formulations (p < 0.05).

whereas protocatechuic acid led to a significant decrease. This could be associated with the different interchain forces and subsequent film compactness established in each case, depending on the molecular structure of phenol. These interaction forces also affected the film flowability and extension during the compression-molding step.

The mechanical properties give essential information for analyzing the strength, stiffness, resistance to break, and extensibility of materials (Liu et al., 2020). The mechanical behavior will be affected by the interactions between the different components of the matrix and the incorporated active compounds (Talón et al., 2017). Table 2 shows the elastic modulus (EM) and tensile strength (TS), and deformation at break (%E) of the different films. The obtained values of tensile parameters for the polyester blend without acids (P) were in the range of those reported by Requena et al. (Requena et al., 2018) for similar polyester blends obtained by melt-blending and compression molding.

The incorporation of phenolic acids significantly (p < 0.05) affected the tensile parameters of the films. Elastic modulus (EM) and tensile strength (TS) increased with the addition of the three acids, higher for protocatechuic acid, which agrees with the above-mentioned more marked interactions of protocatechuic acid with the polymeric chains that limited the crystallization of PHBV (Yen et al., 2008). These results differ from that obtained in other studies carried out with PLA-based films (without PHBV), in which the incorporation of ferulic acid or *p*-coumaric acid led to a decrease in the TS values (Dintcheva et al., 2018; Rigoussen et al., 2018; Sharma et al., 2020). On the other hand, no significant differences in the elongation at break (E) were observed with incorporating the phenolic acids. However, previous studies have shown an increase in extensibility when incorporating ferulic acid into semi-crystalline PLA films (Dintcheva et al., 2018). Therefore, the addition of phenolic acids in the PLA-PHBV matrix resulted in more resistant and stiffer films, which could be attributed to the promoted interactions between phenolic acids and PHBV, but with the same extensibility as the polyester blend (Hernández et al., 2022).

3.3. Barrier properties

Water vapor permeability (WVP) and oxygen permeability (OP) of films conditioned for one week at 25 ºC and 53% RH are shown in Table 2. P films showed WVP values slightly lower than that observed in previous studies (Requena et al., 2018). The incorporation of phenolic compounds in PLA:PHBV polymer matrix reduced the water vapor permeability of the films, probably due to the interaction of the end chain OH groups with acid molecules during the thermal process, which further limits the water solubility in the films and then permeation capability of water molecules. The hydrogen bonding between the phenol groups and oxygen of the polyester group would also affect the

water permeation through the polymer matrix. The slight reported improvement in the water barrier properties was significant (p < 0.05) in films containing protocatechuic acid, coherent with the more marked above-mentioned interactions with PHBV chains.

Likewise, the addition of phenolic acids to the polyester blend led to a significant decrease in oxygen permeability. This improvement was more accentuated for films with protocatechuic acid, coherently with the above-mentioned higher interactions with the polymer chains. Therefore, the decrease in oxygen permeability promoted by phenolic acids can be explained by the interactions between the phenols and polyester chains, tightening the polymer matrix and limiting mass transport phenomena through the films (Benbettaïeb et al., 2019; Contardi et al., 2019).

3.4. Optical properties

Table 2 shows color parameters, internal transmittance, and gloss values (at 60º) for PLA-PHBV blend films with and without phenolic acids. Incorporating phenolic acids promoted slight changes in the color parameters, with total color change (ΔE) inside the non-perceptible range. Likewise, the gloss and internal transmittance (T_i) values of the films slightly increased in films with phenolic acids, especially with the addition of p-coumaric and protocatechuic acids.

The changes in film microstructure and color of the incorporated compounds could cause different light interactions with the films that could affect their optical properties, promoting light scattering or wavelength-selective absorption. Microstructural changes in the film matrix commented on above could affect the light scattering behavior of the films, affecting the film transparency, whereas the colorless nature of the incorporated active compounds would not promote notable changes in the film color and appearance. However, the quantified changes in optical properties were very low given the relatively low concentration of active compounds in the films and their good integration in the polymer matrix.

3.5. Retention of active compounds after film processing and release kinetics

The methanol extraction of phenolic acids from films with ferulic, p-coumaric, and protocatechuic acids and the subsequent quantification by a spectrophotometric method yielded similar values of 83.0 ± 0.03, 80.0 ± 0.1, and 79.0 ± 0.04 g compound retained/100 g compound incorporated, respectively. This decrease in the initially incorporated amount of acids implies a final concentration of 1.7–1.6 g of actives /100 g film, which could be considered enough to inhibit bacterial growth if it is completely released to the food substrate, taking into account the minimal inhibitory concentration of the acids against some bacteria (Table 4). However, the effective release of these compounds into the food substrate is necessary to exert this action. In this sense, analyses of the release kinetics of these active compounds into different
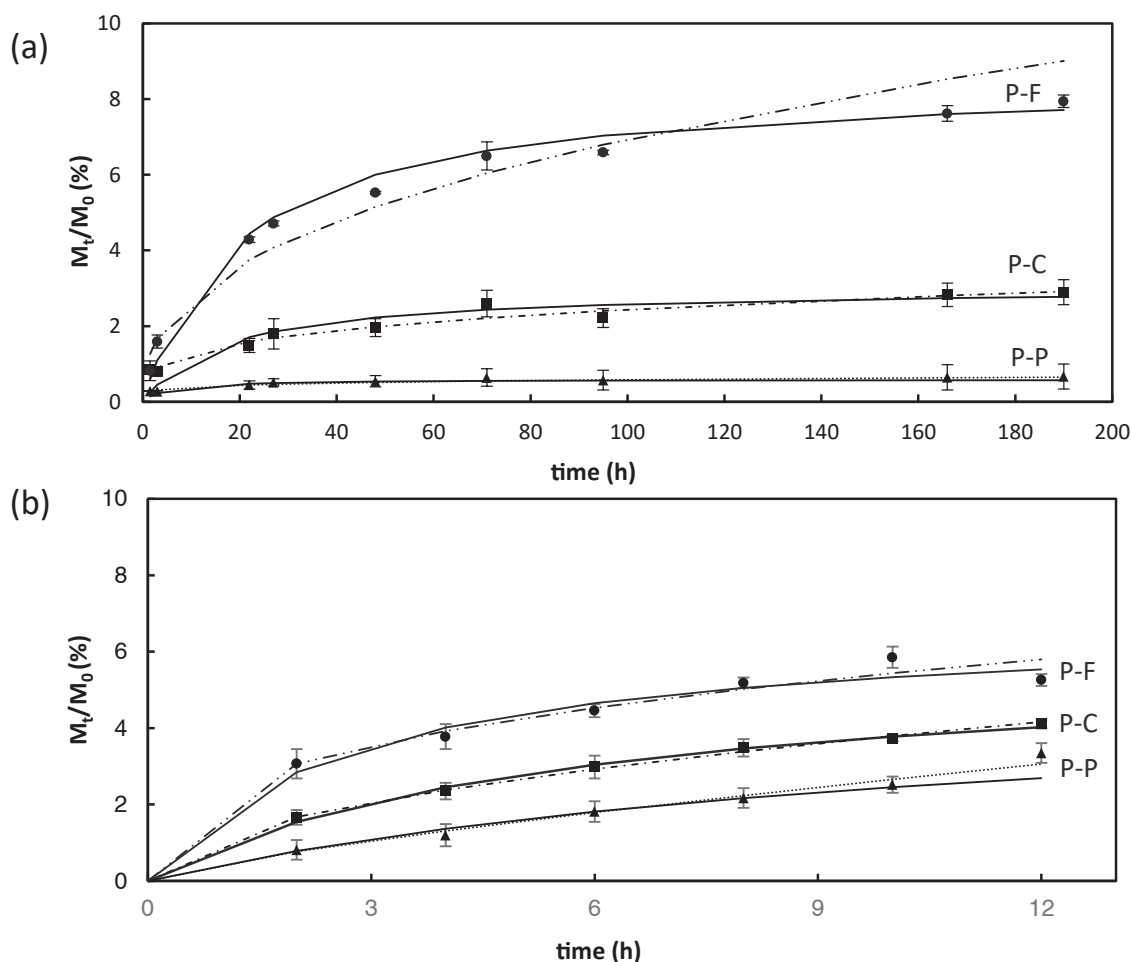

Fig. 4. Values of M_t/M_0 (ratio of the amount of phenolic acid released at each time with respect to the initial mass in the film) as a function of time for the simulant A (a) and simulant D1 (b). Experimental data (points) and Peleg and Korsmeyer-Peppas fitted models (continuous and discontinuous lines, respectively). Values were considered until the film started to disintegrate. Films with ferulic acid (P-F), p-coumaric acid (P-C) and protocatechuic acid (P-P). For Peleg's model R^2 ranged between 0.996 and 0.974 and for Korsmeyer-Peppas R^2 ranged between 0.987 and 0.929 for simulant A and for Peleg's model R^2 ranged between 0.986 and 0.834 and for Korsmeyer-Peppas R^2 ranged between 0.983 and 0.904 for simulant D1.

food simulants (with high and intermediate polarity) were carried out.

Fig. 4 shows the data obtained for the released amount of actives as a function of contact time, for simulants A and D1, respectively, in terms of the M_t/M_0 values (ratio of the amount of phenolic acid released at each time concerning the initial content in the film). The fitted models (Peleg and Korsmeyer-Peppas) were also plotted in Fig. 4. Likewise, Table 3 shows the obtained kinetic parameters from Peleg and Korsmeyer-Peppas models. As expected, different release behavior was observed for the phenolic acids in both simulants according to the different chemical affinity of compounds with the polymer matrix and solubility in both simulants, both factors defining the partition coefficient at equilibrium (Requena et al., 2017). The released ratio of phenolic acids into the simulant D1 (richer in ethanol) was higher than that obtained in simulant A for *p*-coumaric and protocatechuic acids, whereas this was slightly lower for ferulic acid. One important fact was the film's disintegration into the simulants from a determined contact time, depending on the simulant. The kinetic data were only considered up to the disintegration point since from this time the release behavior was accelerated stochastically due to the loss of film integrity. This disintegration occurs faster for films containing acids, whereas the acid-free polyester film remains whole for more than 20 days in contact with both simulants. This suggests that the acid release and the subsequent pH decrease in the aqueous media highly contribute to the film disintegration. The pKa values of the acids are 4.58, 4.64, and 4.26, respectively for ferulic, *p*-coumaric, and protocatechuic acid, and considering the amount released at equilibrium, pH values will be lower than 5 in the aqueous media. However, other authors also observed degradation of PLA films in contact with ethanolic simulants; the higher the ethanol concentration and temperature, the greater the PLA degradation (Jamshidian et al., 2012). Likewise, the release rate of different phenolic antioxidants increased when the ethanol concentration rose, which has been mainly attributed to the penetration of ethanol into the PLA matrix, opening the matrix and favoring the compound diffusion (Mascheroni et al., 2010). Considering the faster release of phenolic acids in D1 simulant (50% aqueous ethanol) and its lower water ratio, a faster pH decrease was expected in this case, thus implying a faster film disintegration. In fact, this disintegration occurred in all acid-loaded films after about 190 h of contact with simulant A (10% aqueous ethanol) and 12 h in contact with simulant D1 (50% aqueous ethanol). Therefore, the asymptotic release value M_∞ (considered as the equilibrium value) was determined from the fitting of Peleg's model to the M_t vs. t data inside the mentioned ranges and considered to calculate the M_t/M_∞ values used to fit the model of Korsmeyer-Peppas.

The highest initial release rate ($1/k_1$) and release ratio at equilibrium was obtained for ferulic acid in the two simulants, whereas protocatechuic acid was the compound most slowly released from the films in both simulants, also reaching the lowest release ratio at equilibrium (0.7% and 5.4% of the film load, in simulants A and D1, respectively). As concerns the effect of simulant, very close values of final release (M_∞/M_0) were obtained for the three acids (6.8–5.4%) in simulant D1, whereas these values differ more in the most polar simulant A. The maximum released amount of the acids was much lower than the compound solubility in water that, in turn, increases with the ethanol content in the simulants. Therefore, the different chemical interactions of the compounds with the polyester matrix and its different degree of

relaxation in contact with the solvent can explain the differences found in the kinetic parameters. In fact, the release rate and the released amount at equilibrium for all phenolic acids were higher in simulant D1, which contained a higher proportion of ethanol, as observed by other authors (Jamshidian et al., 2012) for PLA films. A greater ethanol content promotes PLA relaxation and release of the incorporated compounds.

As concerns the parameters of Korsmeyer-Peppas Model, values of n coefficient were lower than 0.5 in almost all the cases, thus indicating that quasi-Fickian diffusion mechanisms are involved in the release of the three phenolic acids from the PLA:PHBV matrix. Only for protocatechuic acid in simulant D1, n value was higher than 0.5, which is associated with an anomalous transport where diffusion mechanism was coupled with polymer relaxation and swelling caused by the ethanol penetration in the matrix.

From the release study, a very slow release of the active compounds was deduced, highly affected by the polarity of simulant, being non-polar systems, such as fatty foods, those more suitable to favor the delivery of phenolic acids. These systems are more sensitive to oxidation reactions than bacterial growth. Nevertheless, studies in real foods would be necessary to prove the active compound's effectiveness. Next section analyses the antibacterial properties of the phenolic acids and the films containing these, using a gram-positive (*Listeria innocua*) and gram-negative (*Escherichia coli*) bacteria.

3.6. Minimum inhibitory concentration (MIC) of phenolic acids and antibacterial performance of the films

As shown in Table 4, all the used phenolic acids exhibited antibacterial activity against *Escherichia coli* and *Listeria innocua*, with values of

Table 4

Minimum inhibitory concentration (MIC) of the ferulic, *p*-coumaric, and protocatechuic acids studied against *Escherichia coli* and *Listeria innocua*.
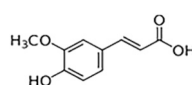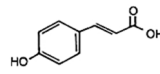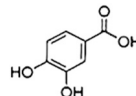
Phenolic acids	MIC (mg/L) *Escherichia coli Listeria innocua*		Other studies (mg/L) *Escherichia coli Listeria innocua*	
Ferulic acid	800	700	> 1000 (Alves et al., 2013)	1942 (Miyague et al., 2015)
			1250 (Borges et al., 2013)	> 1000 (Alves et al., 2013)
p-coumaric acid	800	900	1000 (Alves et al., 2013)	2461 (Miyague et al., 2015)
				> 1000 (Alves et al., 2013)
Protocatechuic acid	750	700	> 1000 (Cueva et al., 2010)	3082 (Miyague et al., 2015)
			1000 (Alves et al., 2013)	1000 (Alves et al., 2013)

Table 3

Parameters of Peleg Model: $1/k_1$ (% released/h); $M_\infty/M_0 = 1/k_2$ (% released at equilibrium) and Korsmeyer-Peppas Model: n (dimensionless) and k (h^{-n}) in simulants A (ethanol aqueous solution, 10% v/v) and D1: (ethanol aqueous solution, 50% v/v). Mean values and standard deviation.

Formulation	Simulant A				Simulant D1			
	Parameters of Peleg Model		Parameters of Korsmeyer-Peppas Model		Parameters of Peleg Model		Parameters of Korsmeyer-Peppas Model	
	$1/k_1$	M_∞/M_0	n	K	$1/k_1$	M_∞/M_0	n	K
P-F	0.4 ± 0.04	8.5 ± 0.4	0.4 ± 0.01	0.13 ± 0.05	2.5 ± 0.6	6.8 ± 0.4	0.4 ± 0.07	0.35 ± 0.06
P-C	0.2 ± 0.04	3.0 ± 0.3	0.3 ± 0.02	0.22 ± 0.07	1.05 ± 0.05	6.0 ± 0.6	0.51 ± 0.05	0.19 ± 0.01
P-P	0.2 ± 0.1	0.7 ± 0.4	0.2 ± 0.1	0.37 ± 0.03	0.46 ± 0.03	5.4 ± 1.5	0.77 ± 0.01	0.08 ± 0.01

MIC ranging from 700 mg/L to 900 mg/L. Protocatechuic acid was the most effective at inhibiting the growth of *Escherichia coli* (lowest MIC) and showed the same MIC as ferulic acid against *Listeria innocua*. The reported MICs values were slightly lower than those found by other authors (Alves et al., 2013; Borges et al., 2013; Cueva et al., 2010; Miyague et al., 2015), which can be explained by changes in the test conditions such as inoculum volume, incubation time, temperature, culture medium, and pH (Pei et al., 2009).

Fig. 5 shows the results of the *in vitro* tests performed with the films in TSB culture medium inoculated with *L. innocua* after 6 days of cold storage. Results showed that the incorporated phenolic acids led to a slight significant decrease ($p < 0.05$) in the growth of *Listeria innocua*, with no significant differences between phenolic acids, whose MIC values were relatively similar. However, the microbial growth inhibition with respect to the polyester films without phenolic acids (P, control) was lower than 2 log CFU, which is what is usually considered as being significant in microbial growth studies. This scarce efficacy of the potentially active films can be explained by the small amount of acid released from the polymeric matrix into the highly polar inoculated culture media, as can be deduced from the release study. In view of these results, antibacterial activity of the films against *E. coli* was not expected, since the MIC values were very similar and were not clearly reached in the medium due to the limited compound delivery from the films. This limited release of the active compounds in aqueous media will also affect the potential antioxidant activity of the films. However, these compounds were effective at preventing fat oxidation in packaged pork meat in this kind of films laminated with starch films (Hernandez et al., 2022).

4. Conclusions

The incorporation of 2% (w/w) of ferulic, *p*-coumaric or protocatechuic acids by melt- blending and compression molding in a polymer matrix of PLA:PHBV (75:25) led to an increase in the glass transition temperature of PLA while PHBV supercooling occurred in the films containing protocatechuic acid. These changes affected the thermal degradation behavior. The addition of ferulic acid increased the thermal stability of the polyester blend films whereas the incorporation of protocatechuic decreased it. Likewise, matrices with phenolic acids were stiffer and more resistant to break than the polyester blend, but with similar extensibility. Oxygen and water vapor barrier capacity were also improved by phenolic acids, in agreement with the higher cohesion forces of the films. Protocatechuic acid promoted the highest effects. The release rate and ratio of phenolic acids increased when the polarity of the food simulant decreases, although very slow delivery was observed in all cases. The three phenolic acids exhibited antibacterial activity against gram-positive (*Listeria innocua)* and gram-negative (*Escherichia coli)* bacteria. However, their incorporation into the polyester blend films did not inhibit significantly the growth of *Listeria innocua* in inoculated culture medium, due to the very limited release of active compounds in the polar culture medium. This would also affect the antioxidant activity of the films since the active compound was not efficiently delivered in aqueous systems. Therefore, the target application of these potentially active packaging materials should consider the scarce release of active compounds in aqueous systems, which will affect the antibacterial performance of the films, although these could act as antioxidant in fatty foods. Further studies are necessary to evaluate other techniques for incorporating the active compounds into the polymeric matrix in order to achieve a more effective release of the active compounds and better antimicrobial performance. Likewise, other active functions of the films, such as the antioxidant capacity, should be evaluated in systems with different polarity.

CRediT authorship contribution statement

Eva Hernández-García: Investigation, Formal analysis, Writing – original draft. **Maria Vargas:** Conceptualization, Methodology, Writing – review & editing, Supervision. **Amparo Chiralt:** Conceptualization, Methodology, Writing – review & editing, Supervision, Funding acquisition.
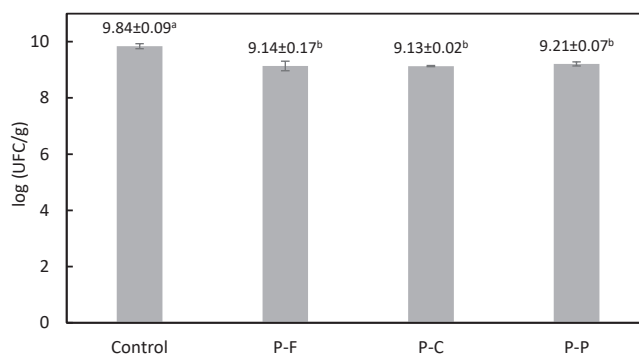
Fig. 5. Microbial counts for *Listeria innocua* obtained after 6 days of incubation to 10 ºC in TSB culture media (in vitro test). Control (P) and PLA-PHBV blend films containing ferulic acid (P-F), *p*-coumaric acid (P-C) and protocatechuic acid (P-P). Mean values ± standard deviation. Different superscript letters (a-b) indicate significant differences among formulations ($p < 0.05$). (Initial inoculum: 10^4 CFU/mL).

References

Alves, M. J., Ferreira, I. C. F. R., Froufe, H. J. C., Abreu, R. M. V., Martins, A., & Pintado, M. (2013). Antimicrobial activity of phenolic compounds identified in wild mushrooms, SAR analysis and docking studies. *Journal of Applied Microbiology, 115* (2), 346–357. https://doi.org/10.1111/jam.12196

Armentano, I., Fortunati, E., Burgos, N., Dominici, F., Luzi, F., Fiori, S., & Kenny, J. M. (2015). Bio-based PLA_PHB plasticized blend films: Processing and structural characterization. *LWT Food Science and Technology, 64*(2), 980–988. https://doi.org/10.1016/j.lwt.2015.06.032

Arrieta, Marina, P., García, A. D., López, D., Fiori, S., & Peponi, L. (2019). Antioxidant bilayers based on PHBV and plasticized electrospun PLA-PHB fibers encapsulating catechin. *Nanomaterials, 9*(3), 1–14. https://doi.org/10.3390/nano9030346

ASTM. (1995). Standard test methods for water vapor transmission of materials. Standard designations: E96-95. *ASTM Annual book of ASTM standards* (pp. 406–413). Philadelphia, PA: American Society fot Testing and Materials.

ASTM. (1999). Standard test method for specular gloss. Standard designations: D523. In *In Annual book of ASTM standards, 06.02.* Philadelphia, PA: American Society for Testing and Materials.

ASTM. (2001). Standard test method for tensile properties of thin plastic sheeting. Standard designations: D882. *Annual book of ASTM standards* (pp. 162–170). Philadelphia, PA: American Society for Testing and Materials.

ASTM. (2002). Standard test method for oxygen gas transmission rate through plastic film and sheeting using a coulometric sensor. Standard designations: 3985-95. *Annual book of ASTM standards* (pp. 472–477). Philadelphia, PA: American Society for Testing and Materials.

Auras, R., Harte, B., & Selke, S. (2004). An overview of polylactides as packaging materials. *Macromolecular Bioscience, 4*(9), 835–864. https://doi.org/10.1002/mabi.200400043

Badui Dergal, S. (2006). Salvador Badui Dergal. *Química de los alimentos* (Fourth ed., p. 2006). México: Pearson Education. ISBN: 970-26-0670-5.

Benbettaïeb, N., Debeaufort, F., & Karbowiak, T. (2019). Bioactive edible films for food applications: Mechanisms of antimicrobial and antioxidant activity. *Critical Reviews in Food Science and Nutrition, 59*(21), 3431–3455. https://doi.org/10.1080/10408398.2018.1494132

Borges, A., Ferreira, C., Saavedra, M. J., & Simões, M. (2013). Antibacterial activity and mode of action of ferulic and gallic acids against pathogenic bacteria. *Microbial Drug Resistance, 19*(4), 256–265. https://doi.org/10.1089/mdr.2012.0244

Castillo, L. A., Farenzena, S., Pintos, E., Rodríguez, M. S., Villar, M. A., García, M. A., & López, O. V. (2017). Active films based on thermoplastic corn starch and chitosan oligomer for food packaging applications. *Food Packaging and Shelf Life, 14*(August), 128–136. https://doi.org/10.1016/j.fpsl.2017.10.004

Chao, C. Y., & Yin, M. C. (2009). Antibacterial effects of roselle calyx extracts and protocatechuic acid in ground beef and apple juice. *Foodborne Pathogens and Disease, 6*(2), 201–206. https://doi.org/10.1089/fpd.2008.0187

Choulitoudi, E., Velliopoulou, A., Tsimogiannis, D., & Oreopoulou, V. (2020). Effect of active packaging with Satureja thymbra extracts on the oxidative stability of fried potato chips. *Food Packaging and Shelf Life, 23*(March 2019), Article 100455. https://doi.org/10.1016/j.fpsl.2019.100455

Contardi, M., Heredia-Guerrero, J. A., Guzman-Puyol, S., Summa, M., Benítez, J. J., Goldoni, L., & Bayer, I. S. (2019). Combining dietary phenolic antioxidants with polyvinylpyrrolidone: Transparent biopolymer films based on: *P*-coumaric acid for controlled release. *Journal of Materials Chemistry B, 7*(9), 1384–1396. https://doi.org/10.1039/c8tb03017k

Cueva, C., Moreno-Arribas, M. V., Martín-Álvarez, P. J., Bills, G., Vicente, M. F., Basilio, A., & Bartolomé, B. (2010). Antimicrobial activity of phenolic acids against commensal, probiotic and pathogenic bacteria. *Research in Microbiology, 161*(5), 372–382. https://doi.org/10.1016/j.resmic.2010.04.006

Dıblan, S., & Kaya, S. (2018). Antimicrobials used in active packaging films. *Food and Health, 4*(1), 63–79. https://doi.org/10.3153/jfhs18007

Dintcheva, N. T., Baiamonte, M., & Spera, M. (2018). Assessment of pro-oxidant activity of natural phenolic compounds in bio-polyesters. *Polymer Degradation and Stability, 152*, 280–288. https://doi.org/10.1016/j.polymdegradstab.2018.05.003

Esmaeili, H., Cheraghi, N., Khanjari, A., Rezaeigolestani, M., Basti, A. A., Kamkar, A., & Aghaee, E. M. (2020). Incorporation of nanoencapsulated garlic essential oil into edible films: A novel approach for extending shelf life of vacuum-packed sausages. *Meat Science, 166*(October 2019), Article 108135. https://doi.org/10.1016/j.meatsci.2020.108135

Ferreira, B. M. P., Zavaglia, C. A. C., & Duek, E. A. R. (2002). Films of PLLA/PHBV: Thermal, morphological, and mechanical characterization. *Journal of Applied Polymer Science, 86*(11), 2898–2906.

Figueroa-Lopez, K. J., Cabedo, L., Lagaron, J. M., & Torres-Giner, S. (2020). Development of electrospun Poly(3-hydroxybutyrate-co-3-hydroxyvalerate) monolayers containing eugenol and their application in multilayer antimicrobial food packaging. *Frontiers in Nutrition, 7*(September), 1–16. https://doi.org/10.3389/fnut.2020.00140

Furukawa, T., Sato, H., Murakami, R., Zhang, J., Duan, Y. X., Noda, I., & Ozaki, Y. (2005). Structure, dispersibility and crystallinity of poly (hydroxybutyrate)/ poly(l-lactic acid) blends studied by FT-IR microspectroscopy and differential scanning calorimetry. *Macromolecules, 38*(15), 6445–6454. https://doi.org/10.1021/ma0504668

González-Ausejo, J., Sánchez-Safont, E., Lagarón, J. M., Balart, R., Cabedo, L., & Gámez-Pérez, J. (2017). Compatibilization of poly(3-hydroxybutyrate-co-3-hydroxyvalerate)–poly(lactic acid) blends with diisocyanates. *Journal of Applied Polymer Science, 134*(20), 1–11. https://doi.org/10.1002/a

Hernández-García, E., Vargas, M., & Chiralt, A. (2021). Thermoprocessed starch-polyester bilayer films as affected by the addition of gellan or xanthan gum. *Food Hydrocolloids, 113*(December 2020). https://doi.org/10.1016/j.foodhyd.2020.106509

Hutchings, J. B. (1999). *Food and colour appearance* (second ed.). Gaithersburg, Maryland: Chapman and Hall Food Science Book, Aspen Publication.

Jamshidian, M., Arab Tehrany, E., & Desobry, S. (2012). Release of synthetic phenolic antioxidants from extruded poly lactic acid (PLA) film. *Food Control, 28*, 445–455. https://doi.org/10.1016/j.foodcont.2012.05.005

Jiang, J., Gong, L., Dong, Q., Kang, Y., Osako, K., & Li, L. (2020). Characterization of PLA-P3,4HB active film incorporated with essential oil: Application in peach preservation. *Food Chemistry, 313*((November 2019). https://doi.org/10.1016/j.foodchem.2019.126134

Kanda, G. S., Al-Qaradawi, I., & Luyt, A. S. (2018). Morphology and property changes in PLA/PHBV blends as function of blend composition. *Journal of Polymer Research, 25*(9). https://doi.org/10.1007/s10965-018-1586-3

Kasmi, S., Gallos, A., Beaugrand, J., Paës, G., & Allais, F. (2019). Ferulic acid derivatives used as biobased powders for a convenient plasticization of polylactic acid in continuous hot-melt process. *European Polymer Journal, 110*(March 2018), 293–300. https://doi.org/10.1016/j.eurpolymj.2018.11.036

Krepker, M., Shemesh, R., Danin Poleg, Y., Kashi, Y., Vaxman, A., & Segal, E. (2017). Active food packaging films with synergistic antimicrobial activity. *Food Control, 76*, 117–126. https://doi.org/10.1016/j.foodcont.2017.01.014

Liu, Q., Wu, C., Zhang, H., & Deng, B. (2015). Blends of polylactide and poly(3-hydroxybutyrate-co-3-hydroxyvalerate) with low content of hydroxyvalerate unit: Morphology, structure, and property. *Journal of Applied Polymer Science, 132*(42), 1–9. https://doi.org/10.1002/a

Liu, W., Wang, Z., Liu, J., Dai, B., Hu, S., Hong, R., & Zeng, G. (2020). Preparation, reinforcement and properties of thermoplastic starch film by film blowing. *Food Hydrocolloids, 108*(February), Article 106006. https://doi.org/10.1016/j.foodhyd.2020.106006

Lou, Z., Wang, H., Rao, S., Sun, J., Ma, C., & Li, J. (2012). *P*-Coumaric acid kills bacteria through dual damage mechanisms. *Food Control, 25*(2), 550–554. https://doi.org/10.1016/j.foodcont.2011.11.022

Malhotra, B., Keshwani, A., & Kharkwal, H. (2015). Antimicrobial food packaging: Potential and pitfalls. *Frontiers in Microbiology, 6*(JUN), 1–9. https://doi.org/10.3389/fmicb.2015.00611

Mascheroni, E., Guillard, V., Nalin, F., Mora, L., & Piergiovanni, L. (2010). Diffusivity of propolis compounds in polylactic acid polymer for the development of antimicrobial packaging films. *Journal of Food Engineering, 98*, 294–301. https://doi.org/10.1016/j.jfoodeng.2009.12.028

Mathew, S., & Abraham, T. E. (2008). Characterisation of ferulic acid incorporated starch-chitosan blend films. *Food Hydrocolloids, 22*(5), 826–835. https://doi.org/10.1016/j.foodhyd.2007.03.012

Mitani, T., Ota, K., Inaba, N., Kishida, K., & Koyama, H. A. (2018). Antimicrobial activity of the phenolic compounds of Prunus mume against enterobacteria. *Biological and Pharmaceutical Bulletin, 41*(2), 208–212. https://doi.org/10.1248/bpb.b17-00711

Miyague, L., Macedo, R. E. F., Meca, G., Holley, R. A., & Luciano, F. B. (2015). Combination of phenolic acids and essential oils against *Listeria monocytogenes*. *LWT - Food Science and Technology, 64*(1), 333–336. https://doi.org/10.1016/j.lwt.2015.05.055

Mohan, V., Wibisono, R., de Hoop, L., Summers, G., & Fletcher, G. C. (2019). Identifying suitable *Listeria innocua* strains as surrogates for *Listeria monocytogenes* for horticultural products. *Frontiers in Microbiology, 10*, 2281. https://doi.org/10.3389/fmicb.2019.02281

Moreno, O., Atarés, L., Chiralt, A., Cruz-Romero, M. C., & Kerry, J. (2018). Starch-gelatin antimicrobial packaging materials to extend the shelf life of chicken breast fillets. *Lwt, 97*(February), 483–490. https://doi.org/10.1016/j.lwt.2018.07.005

Moreno, S., Scheyer, T., Romano, C. S., & Vojnov, A. A. (2006). Antioxidant and antimicrobial activities of rosemary extracts linked to their polyphenol composition. *Free Radical Research, 40*(2), 223–231. https://doi.org/10.1080/10715760500473834

Muller, J., González-Martínez, C., & Chiralt, A. (2017). Poly(lactic) acid (PLA) and starch bilayer films, containing cinnamaldehyde, obtained by compression moulding. *European Polymer Journal, 95*(July), 56–70. https://doi.org/10.1016/j.eurpolymj.2017.07.019

Narasagoudr, S. S., Hegde, V. G., Chougale, R. B., Masti, S. P., & Dixit, S. (2020). Influence of boswellic acid on multifunctional properties of chitosan/poly (vinyl alcohol) films for active food packaging. *International Journal of Biological Macromolecules, 154*, 48–61. https://doi.org/10.1016/j.ijbiomac.2020.03.073

Ngo, T. M. P., Nguyen, T. H., Dang, T. M. Q., Tran, T. X., & Rachtanapun, P. (2020). Characteristics and antimicrobial properties of active edible films based on pectin and nanochitosan. *International Journal of Molecular Sciences, 21*(6). https://doi.org/10.3390/ijms21062224

Noda, I., Satkowski, M. M., Dowrey, A. E., & Marcott, C. (2004). Polymer alloys of nodax copolymers and poly(lactic acid). *Macromolecular Bioscience, 4*(3), 269–275. https://doi.org/10.1002/mabi.200300093

Nuchanong, P., Seadan, M., Khankrua, R., & Suttiruengwong, S. (2021). Thermal stability enhancement of poly(hydroxybutyrate-co-hydroxyvalerate) through in situ reaction. *Designed Monomers and Polymers, 24*(1), 113–124. https://doi.org/10.1080/15685551.2021.1914406

Pei, R. S., Zhou, F., Ji, B. P., & Xu, J. (2009). Evaluation of combined antibacterial effects of eugenol, cinnamaldehyde, thymol, and carvacrol against E. coli with an improved method. *Journal of Food Science, 74*(7), 379–383. https://doi.org/10.1111/j.1750-3841.2009.01287.x

Peleg, M. (1988). An empirical model for the description of moisture sorption curves. *Journal of Food Science, 53*(4), 1216–1217. https://doi.org/10.1111/j.1365-2621.1988.tb13565.x

Porras-Loaiza and López-Malo. (2009). Importancia de los grupos fenólicos en los alimentos. *In Temas Selectos de Ingeniería de Alimentos* (Vol. 3, Issue 1, pp. 121–134). https://www.udlap.mx/WP/tsia/files/No3-Vol-1/TSIA-3(1)-Porras-Loaiza-et-al-2009.pdf.

Quiles-Carrillo, L., Montanes, N., Pineiro, F., Jorda-Vilaplana, A., & Torres-Giner, S. (2018). Ductility and toughness improvement of injection-molded compostable pieces of polylactide by melt blending with poly(ε-caprolactone) and thermoplastic starch. *Materials, 11*(11), 2138. https://doi.org/10.3390/ma11112138

Requena, R., Vargas, M., & Chiralt, A. (2017). Release kinetics of carvacrol and eugenol from poly(hydroxybutyrate-co-hydroxyvalerate) (PHBV) films for food packaging applications. *European Polymer Journal, 92*(May), 185–193. https://doi.org/10.1016/j.eurpolymj.2017.05.008

Requena, R., Vargas, M., & Chiralt, A. (2018). Obtaining antimicrobial bilayer starch and polyester-blend films with carvacrol. *Food Hydrocolloids, 83*, 118–133. https://doi.org/10.1016/j.foodhyd.2018.04.045

Requena, R., Vargas, M., & Chiralt, A. (2019). Study of the potential synergistic antibacterial activity of essential oil components using the thiazolyl blue tetrazolium bromide (MTT) assay. *Lwt, 101*(June 2018), 183–190. https://doi.org/10.1016/j.lwt.2018.10.093

Requena, R., Jiménez, A., Vargas, M., & Chiralt, A. (2016). Effect of plasticizers on thermal and physical properties of compression-moulded poly[(3-hydroxybutyrate)-co- (3-hydroxyvalerate)] films. *Polymer Testing, 56*, 45–53. https://doi.org/10.1016/j.polymertesting.2016.09.022

Rigoussen, A., Verge, P., Raquez, J. M., & Dubois, P. (2018). Natural phenolic antioxidants as a source of biocompatibilizers for immiscible polymer blends. *ACS Sustainable Chemistry and Engineering, 6*(10), 13349–13357. https://doi.org/10.1021/acssuschemeng.8b02999

Sharma, S., Jaiswal, A. K., Duffy, B., & Jaiswal, S. (2020). Ferulic acid incorporated active films based on poly(lactide) /poly(butylene adipate-co-terephthalate) blend for food packaging. *Food Packaging and Shelf Life, 24*(October 2019). https://doi.org/10.1016/j.fpsl.2020.100491

Siepmann, J., & Peppas, N. A. (2011). Higuchi equation: Derivation, applications, use and misuse. *International Journal of Pharmaceutics, 418*(1), 6–12. https://doi.org/10.1016/j.ijpharm.2011.03.051

Siepmann, J., & Peppas, N. A. (2012). Modeling of drug release from delivery systems based on hydroxypropyl methylcellulose (HPMC). *Advanced Drug Delivery Reviews, 64*(SUPPL), 163–174. https://doi.org/10.1016/j.addr.2012.09.028

Snowdon, M. R., Mohanty, A. K., & Manjusri Misra, M. (2017). Miscibility and performance evaluation of biocomposites made from polypropylene/poly(lactic acid)/Poly(hydroxybutyrate-co-hydroxyvalerate) with a sustainable biocarbon filler. *ACS Omega, 2*(10), 6446–6454. https://doi.org/10.1021/acsomega.7b00983

Stojković, D. S., Živković, J., Soković, M., Glamočlija, J., Ferreira, I. C. F. R., Janković, T., & Maksimović, Z. (2013). Antibacterial activity of Veronica montana L. extract and of protocatechuic acid incorporated in a food system. *Food and Chemical Toxicology, 55*, 209–213. https://doi.org/10.1016/j.fct.2013.01.005

Szabo, K., Teleky, B. E., Mitrea, L., Călinoiu, L. F., Martău, G. A., Simon, E., & Vodnar, D. C. (2020). Active packaging-poly (vinyl alcohol) films enriched with tomato by-products extract. *Coatings, 10*(2), 1–18. https://doi.org/10.3390/coatings10020141

Takahashi, H., Kashimura, M., Koiso, H., Kuda, T., & Kimura, B. (2013). Use of ferulic acid as a novel candidate of growth inhibiting agent against Listeria monocytogenes in ready-to-eat food. *Food Control, 33*(1), 244–248. https://doi.org/10.1016/j.foodcont.2013.03.013

Takahashi, H., Takahashi, T., Miya, S., Yokoyama, H., Kuda, T., & Kimura, B. (2015). Growth inhibition effects of ferulic acid and glycine/sodium acetate onListeria monocytogenes in coleslaw and egg salad. *Food Control, 57*, 105–109. https://doi.org/10.1016/j.foodcont.2015.03.037

Talón, E., Trifkovic, K. T., Nedovic, V. A., Bugarski, B. M., Vargas, M., Chiralt, A., & González-Martínez, C. (2017). Antioxidant edible films based on chitosan and starch containing polyphenols from thyme extracts. *Carbohydrate Polymers, 157*, 1153–1161. https://doi.org/10.1016/j.carbpol.2016.10.080

Valencia-Sullca, C., Jiménez, M., Jiménez, A., Atarés, L., Vargas, M., & Chiralt, A. (2016). Influence of liposome encapsulated essential oils on properties of chitosan films. *Polymer International, 65*(8), 979–987. https://doi.org/10.1002/pi.5143

Vargas, M., Chiralt, A., Albors, A., & González-Martínez, C. (2009). Effect of chitosan-based edible coatings applied by vacuum impregnation on quality preservation of fresh-cut carrot. *Postharvest Biology and Technology, 51*(2), 263–271. https://doi.org/10.1016/j.postharvbio.2008.07.019

Wang, L., Dekker, M., Heising, J., Fogliano, V., & Berton-Carabin, C. C. (2020). Carvacrol release from PLA to a model food emulsion: Impact of oil droplet size. *Food Control, 114*(January), Article 107247. https://doi.org/10.1016/j.foodcont.2020.107247

Yen, K. C., Mandal, T. K., & Woo, E. M. (2008). Enhancement of bio-compatibility via specific interactions in polyesters modified with a bio-resourceful macromolecular ester containing polyphenol groups. *Journal of Biomedical Materials Research Part A, 86*(3), 701–712.

Zembouai, I., Kaci, M., Bruzaud, S., Benhamida, A., Corre, Y. M., & Grohens, Y. (2013). A study of morphological, thermal, rheological and barrier properties of Poly(3-hydroxybutyrate-Co-3-Hydroxyvalerate)/polylactide blends prepared by melt mixing. *Polymer Testing, 32*(5), 842–851. https://doi.org/10.1016/j.polymertesting.2013.04.004

Zhang, H., Liang, Y., Li, X., & Kang, H. (2020). Effect of chitosan-gelatin coating containing nano-encapsulated tarragon essential oil on the preservation of pork slices. *Meat Science, 166*(February), Article 108137. https://doi.org/10.1016/j.meatsci.2020.108137

Zhang, H. Y., Arab Tehrany, E., Kahn, C. J. F., Ponot, M., Linder, M., & Cleymand, F. (2012). Effects of nanoliposomes based on soya, rapeseed and fish lecithins on chitosan thin films designed for tissue engineering. *Carbohydrate Polymers, 88*(2), 618–627. https://doi.org/10.1016/j.carbpol.2012.01.007

Zhao, H., Cui, Z., Sun, X., Turng, L. S., & Peng, X. (2013). Morphology and properties of injection molded solid and microcellular polylactic acid/polyhydroxybutyrate-valerate (PLA/PHBV) blends. *Industrial & Engineering Chemistry Research, 52*(7), 2569–2581.